

19. W. von Maier, *Zool. Syst. Evolutionsforsch.* **27**, 149 (1989).

20. _____, in *Mammal Phylogeny*, F. S. Szalay, M. J. Novacek, M. C. McKenna, Eds. (Springer-Verlag, New York, 1993), pp. 165–181.

21. U. Zeller, in *Morphogenesis of the Mammalian Skull*, H.-J. Kuhn, U. Zeller, Eds. (Parey, Hamburg, 1987), pp. 17–50.

22. Supplementary data are available on Science Online at www.sciencemag.org/cgi/content/full/292/5521/1535/DC1.

23. J. A. Lillegraven, G. Krusat, *Contrib. Geol. Univ. Wyo.* **28**, 39 (1991).

24. T. S. Kemp, *Mammal-Like Reptiles and Origin of Mammals* (Academic Press, London, 1982), pp. 1–363.

25. J. A. Hopson, H. R. Barghusen, in *The Ecology and Biology of Mammal-Like Reptiles*, N. Hotton III, P. D. MacLean, J. J. Roth, E. C. Roth, Eds. (Smithsonian Institution Press, Washington, DC, 1986), pp. 83–106.

26. E. F. Allin, J. A. Hopson, in *The Evolutionary Biology of Hearing*, D. B. Webster, R. R. Fay, A. N. Popper, Eds. (Springer-Verlag, New York, 1992), pp. 587–614.

27. Z.-X. Luo, in *In the Shadow of Dinosaurs—Early Mesozoic Tetrapods*, N. C. Fraser, H.-D. Sues, Eds. (Cambridge Univ. Press, Cambridge, 1994), pp. 98–128.

28. R. L. Cifelli, J. R. Wible, F. A. Jenkins Jr., *J. Vertebr. Paleontol.* **18**, 237 (1998).

29. Q. Ji, Z.-X. Luo, S.-A. Ji, *Nature* **398**, 326 (1999).

30. Y.-M. Hu, Y.-Q. Wang, Z.-X. Luo, C.-K. Li, *Nature* **390**, 137 (1997).

31. Z. Kielan-Jaworowska, *Lethaia* **29**, 249 (1997).

32. _____, *Contrib. Geol. Univ. Wyo.* **3**, 21 (1986).

33. T. Rowe, *Science* **273**, 651 (1996).

34. H. J. Jerison, *Evolution of the Brain and Intelligence* (Academic Press, New York, 1973).

35. G. Hahn, *Palaeovertebrata* **18**, 155 (1988).

36. Z. Kielan-Jaworowska, J. H. Hurum, *Acta Palaeontol. Pol.* **42**, 201 (1997).

37. A. M. Musser, M. Archer, *Philos. Trans. R. Soc. London Ser. B* **353**, 1063 (1998).

38. Z.-X., Luo, A. W. Crompton, S. G. Lucas, *J. Vertebr. Paleontol.* **15**, 113 (1995).

39. J. R. Wible, J. A. Hopson, in *Mammal Phylogeny*, F. S. Szalay, M. J. Novacek, M. C. McKenna, Eds. (Springer-Verlag, New York, 1993), pp. 45–62.

40. G. W. Rougier, J. R. Wible, J. A. Hopson, *Am. Mus. Novitates* **3183**, 1 (1996).

41. Z.-X. Luo, A. W. Crompton, *J. Vertebr. Paleontol.* **14**, 341 (1994).

42. T. Rowe, *J. Vertebr. Paleontol.* **8**, 241 (1988).

43. C. A. Sidor, J. A. Hopson, *Paleobiology* **24**, 254 (1998).

44. The negative allometry of the middle ear bones relative to the whole skull during development of *Monodelphis* is consistent with the observation of monotremes and some eutherians. During the development of *Ornithorhynchus* (17, 18), the malleus shows negative allometry relative to the overall growth of the entire skull. As the posterior Meckel's cartilage is ossified and transformed into the malleus, the diameter of the arc between the anterior process of the malleus and the manubrium increases by only 25% (from 3 to ~4 mm) as the skull length increases by almost 300% (from 24 to 106 mm). The placental *Tupaia* (21) has a substantial growth in skull size after the ossification and fixation of size of the middle ear structure.

45. S. Nummela, *Theor. Biol.* **4**, 387 (1997).

46. K. K. Smith, *Evolution* **51**, 1663 (1997).

47. Differentiation of the central nervous system in eutherians (21, 46) occurs in advance of the ossification of TMJ, which, in turn, occurs before the ossification of middle ear ossicles (21, 46). The sequence of these events is the opposite that of marsupials, indicating an unambiguous case of heterochrony among living therians [(46), and references cited therein]. The dentary/squamosal joint is also established earlier than ossification of the middle ear ossicles in monotremes (16–18), similar to placentals but different from marsupials [(19, 20) and references cited therein]. The Meckel's cartilage and its derivative elements (the incus and malleus) are positioned on the basicranium and well separated from the dentary in early ontogeny in eutherians (21). This is different from marsupials, in which the Meckel's cartilage and its derivative elements are closely attached to the dentary until the final separation from the latter in a later postnatal stage (19, 20).

48. S. W. Herring, *Am. Zool.* **33**, 472 (1993).

49. Teratological evidence shows that masticatory muscle attachment to the Meckel's cartilage in abnormal human development can delay its reabsorption (48). Thus, reabsorption of the Meckel's cartilage may be associated with the loss of mechanical stress and loading as the masticatory muscles shifted their attachment from Meckel's cartilage to the dentary during normal development (48). Maier (19, 20) also proposed that movement of the dentary during suckling would result in disruption of the Meckel's cartilage.

50. P. D. Gingerich, B. H. Smith, in *Size and Scaling in Primate Biology*, W. L. Jungers, Ed. (Plenum, New York, 1984), pp. 257–272.

51. J. I. Bloch, K. D. Rose, P. D. Gingerich, *J. Mammal.* **79**, 804 (1998).

52. J. Alroy, *Science* **280**, 731 (1998).

53. B. Van Valkenburgh, *Trends Ecol. Evol.* **10**, 71 (1995).

54. J. Jernvall, J. P. Hunter, M. Fortelius, *Science* **252**, 1831 (1996).

55. M. Foote, *Annu. Rev. Ecol. Syst.* **28**, 129 (1997).

56. We thank W. W. Amaral for a superb preparation; M. Klingler for graphics; J. Suhan for photography; A. Henrici for assistance; F. A. Jenkins, J. R. Wible, G.-H. Cui, and F.-K. Zhang for access to the comparative collections; P. D. Gingerich for generously providing body mass/skull measurements of extant insectivores; J. Alroy, K. C. Beard, M. R. Dawson, P. D. Gingerich, Z. Kielan-Jaworowska, T. Rowe, K. K. Smith, J. G. M. Thewissen, and J. R. Wible for discussion; and M. R. Dawson, J. A. Hopson, Z. Kielan-Jaworowska, and J. R. Wible for improving the paper. Research supported by the CAREER award of NSF (DEB 95278902), National Geographic Society (grant 5338-94), and Carnegie Museum (Z.-X.L.), and NIH and Harvard University (A.W.C.).

20 December 2000; accepted 15 March 2001

Chromatin Docking and Exchange Activity Enhancement of RCC1 by Histones H2A and H2B

Michael E. Nemerlut,^{1,2*}† Craig A. Mizzen,⁴ Todd Stukenberg,⁴ C. David Allis,⁴ Ian G. Macara^{1,3}

The Ran guanosine triphosphatase (GTPase) controls nucleocytoplasmic transport, mitotic spindle formation, and nuclear envelope assembly. These functions rely on the association of the Ran-specific exchange factor, RCC1 (regulator of chromosome condensation 1), with chromatin. We find that RCC1 binds directly to mononucleosomes and to histones H2A and H2B. RCC1 utilizes these histones to bind *Xenopus* sperm chromatin, and the binding of RCC1 to nucleosomes or histones stimulates the catalytic activity of RCC1. We propose that the docking of RCC1 to H2A/H2B establishes the polarity of the Ran-GTP gradient that drives nuclear envelope assembly, nuclear transport, and other nuclear events.

RCC1 can be considered as a chromatin marker. Catalysis of guanine nucleotide exchange on Ran by RCC1 to produce Ran-GTP is essential for mitotic spindle assembly and nuclear envelope formation (1–4). Once enclosed by the envelope, chromatin-bound

RCC1 generates a Ran-GTP gradient across nuclear pores that permits vectorial nucleocytoplasmic transport (4). The docking mechanism for RCC1 onto chromatin is unknown. RCC1 may bind DNA in vitro, but removal of the NH₂-terminal domain of

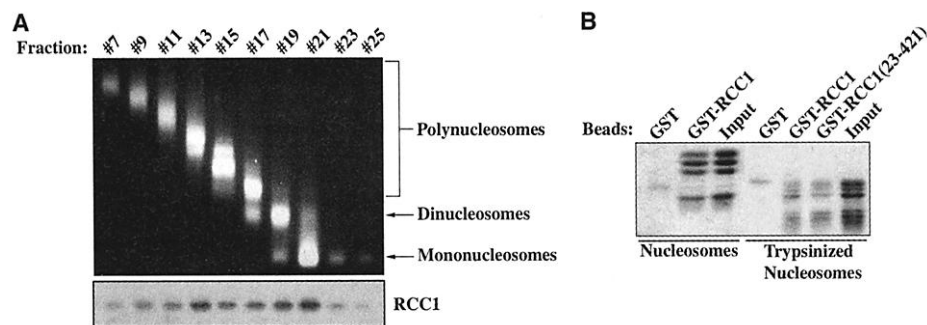


Fig. 1. RCC1 binds mononucleosomes. (A) HeLa nuclei were digested with micrococcal nuclease and centrifuged through a linear 8 to 20% sucrose gradient. Samples of individual fractions were electrophoresed through a tris-borate EDTA-agarose gel and visualized by ethidium bromide staining (top) or precipitated with trichloroacetic acid, subjected to SDS-PAGE, and immunoblotted (N-19, Santa Cruz) for endogenous RCC1 (bottom). (B) Immobilized GST, GST-RCC1, or GST-RCC1(23–421) was incubated with intact or trypsinized H1-depleted mononucleosomes. After washing, proteins were eluted, subjected to SDS-PAGE, and stained with Coomassie.

REPORTS

RCC1 abrogates DNA binding without loss of *in vivo* chromatin association (5).

To identify the mechanism for chromatin binding, HeLa nuclei were partially digested with micrococcal nuclease and the solubilized chromatin was separated by centrifugation (6). The majority of RCC1 cosedimented with nucleosomal fractions (Fig. 1A), suggesting that endogenous RCC1 associates with nucleosomes. Glutathione *S*-transferase (GST)-tagged RCC1 (GST-RCC1), but not GST, bound H1-depleted mononucleosomes (6), demonstrating a direct interaction (Fig. 1B) (7). The core histones have folded regions that participate in octamer assembly and DNA binding as well as highly modified NH₂-terminal tails (8). Brief treatment with trypsin digests these NH₂-terminal tails while leaving the folded domains intact. GST-RCC1 bound both intact and trypsinized mononucleosomes (Fig. 1B) (7). Binding of GST-RCC1 to recombinant histone tails from H2B and H3 was barely detectable (9). Thus, the histone tails may contribute to, but are not necessary for, the binding of RCC1 to chromatin.

Association of RCC1 with nucleosomes could be mediated by binding to DNA, histones, or both components; however, a mutant RCC1 lacking its DNA binding region [GST-RCC1(23-421)] retained its ability to associate with trypsinized nucleosomes (Fig. 1B). To determine whether RCC1 binds directly to histones, immobilized GST or GST-RCC1 was incubated with histones from chicken erythrocyte nuclei (7). In this experiment, we presume that H2A/H2B assemble heterodimers that are not associated with the H3/H4 heterotetramers (10). GST-RCC1 depleted all four histones from the supernatant (Fig. 2A); however, H3/H4 were removed during the washes and only H2A/H2B remained bound. Thus, RCC1 binds directly to histones, and preferentially to H2A/H2B.

Ran-GTP regulates the interaction of nuclear transport receptors with their cargoes. To determine whether Ran also regulates the histone-RCC1 interaction, the binding assay was repeated with an excess of wild-type or one of two mutant forms of Ran (7). Ran(T24N) has a reduced ability to bind nucleotide but increased affinity for RCC1; Ran(Q69L) is constitutively GTP-bound (11, 12). These forms of Ran did not decrease RCC1 binding to H2A/H2B (Fig. 2A), suggesting that Ran does not disrupt the binding of RCC1 to chromatin.

Because H2A and H2B heterodimerize, RCC1 could interact with either protein alone, or only with the heterodimer. GST-RCC1 bound H2A or H2B alone even when their concentration was only 50 nM (Fig. 2B), suggesting that RCC1 associates tightly with either histone in the absence of DNA.

Because the interaction between RCC1

and H2A/H2B was not competitive with Ran binding, we expected that chromatin-bound RCC1 would catalyze nucleotide exchange. Therefore, exchange reactions were performed (13) with or without H2A/H2B or H3/H4. The addition of H2A/H2B stimulated the catalytic activity of RCC1 (Fig. 2, C and D), increasing the dissociation rate constant,

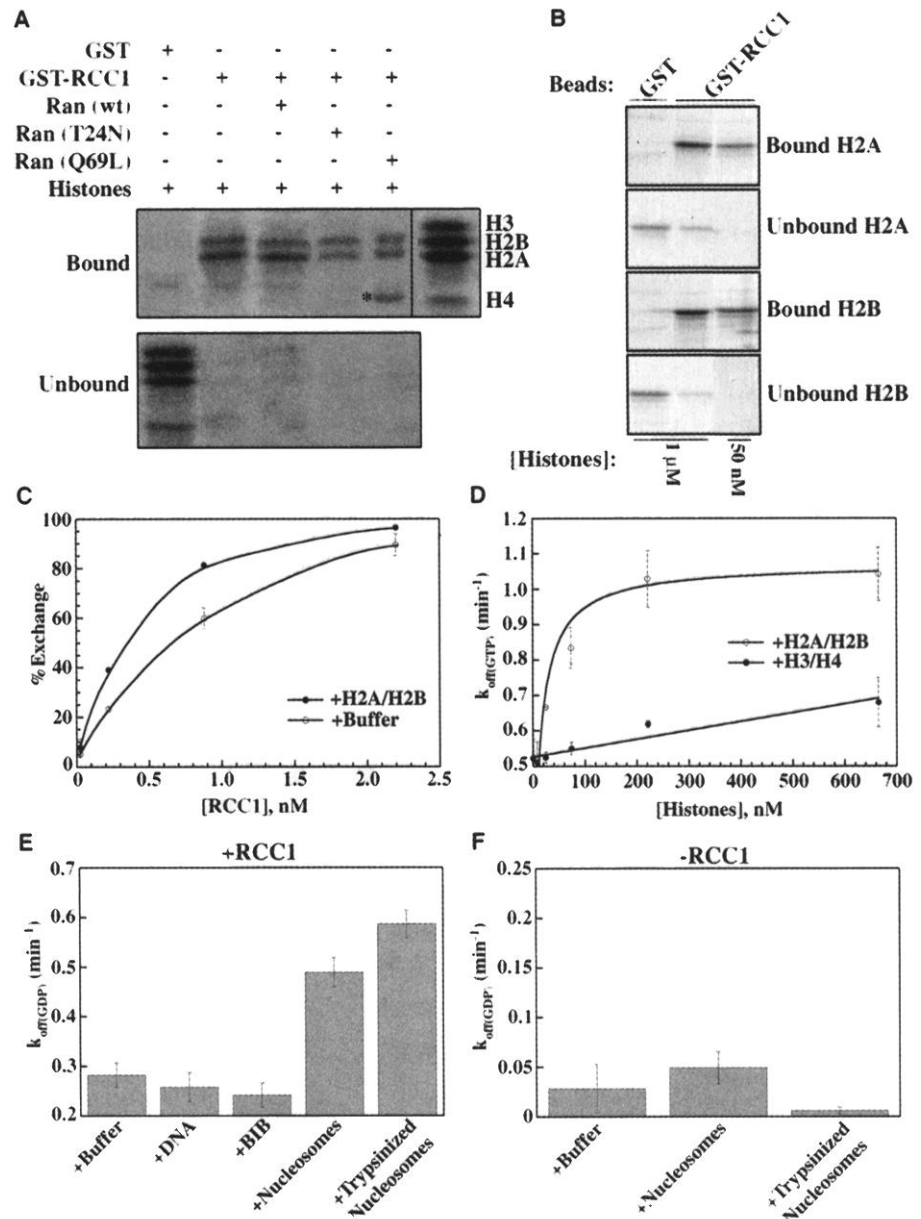


Fig. 2. Histones bind directly to RCC1 and enhance its catalytic activity. (A) Immobilized GST or GST-RCC1 (1 μ M) was incubated with chicken histones (1 μ M) with (+) or without (-) the indicated form of Ran (10 μ M). Histones in the unbound fraction were isolated with SP-Sephadex beads (Pharmacia). Bound and unbound fractions were subjected to SDS-PAGE and stained with Coomassie. The asterisk indicates a degradation product from Ran(Q69L), not histone H4. (B) As in (A), except that H2A or H2B was used. (C) Exchange reactions were performed with or without H2A/H2B (333 nM). Samples were analyzed by binding to nitrocellulose and scintillation counting. (D) As in (C), except that a fixed concentration of RCC1 (0.9 nM) was used with various concentrations of H2A/H2B or H3/H4 (Roche). Reactions were performed with (E) or without (F) RCC1 (0.9 nM), with or without DNA, BIB domain, nucleosomes, or trypsinized nucleosomes (all 250 nM). Dissociation rate constants were calculated assuming first-order kinetics (24). Error bars represent the range from the mean ($n = 2$). Data are representative of at least three independent experiments.

¹Center for Cell Signaling, ²Department of Microbiology, ³Department of Pharmacology, ⁴Department of Biochemistry, University of Virginia, Charlottesville, VA 22908, USA.

*To whom correspondence should be addressed. E-mail: men5w@virginia.edu

†Present address: University of Virginia, Hospital West RM 7191, Post Office Box 800577 HSC, Charlottesville, VA 22908.

REPORTS

k_{off} , for nucleotide by \sim twofold (Fig. 2C). The effect was saturable, with an apparent dissociation equilibrium constant $K_{1/2}$, of \sim 25 nM. H2A and H2B stimulated RCC1 individually and enhanced exchange of guanosine diphosphate (GDP) for GTP or vice versa; the NH_2 -terminal tails from H2A/H2B did not stimulate RCC1 (9). The beta-like import receptor-binding (BIB) domain, a basic protein fragment derived from ribosomal protein L23a (4), also did not stimulate RCC1, demonstrating that the effect was histone-specific and not merely a consequence of positive charge (Fig. 2E). In addition, the histones H3/H4 only stimulated RCC1 weakly and at high concentrations (Fig. 2D). Intact and trypsinized RCC1-depleted mononucleosomes (Fig. 2F) stimulated exchange similarly to H2A/H2B (Fig. 2, D and E), with a $K_{1/2}$ of \sim 100 nM (14), whereas DNA itself had no effect (Fig. 2E). Taken together, these data suggest that H2A/H2B are cofactors for RCC1 at the chromatin surface.

It was important to determine whether RCC1 utilizes H2A/H2B for chromatin binding in vivo. Therefore, we used chromatin isolated from the sperm of *Xenopus laevis* that are deficient in histones H2A/H2B (15–17). *Xenopus* sperm are the only known cells in which RCC1 is not predominantly chromatin-bound (18).

When added to egg lysate, *Xenopus* sperm undergo two decondensation reactions (19). During stage I decondensation (\sim 10 min), nucleoplasmic core (NpIC) replaces sperm-specific basic proteins (X and Y) with H2A/H2B (16, 17). The addition of a membrane fraction permits stage II decondensation which includes pronucleus formation. Because RCC1 is required for nuclear envelope assembly (1, 2), it must mobilize to chromatin during either stage I or early stage II decondensation. The level of endogenous RCC1 on demembrated sperm chromatin was too low to be detectable; however, within 10 min after the addition of egg extract, RCC1 relocalized to the nuclear pellet (Fig. 3A, top) (20). To observe chromatin binding of RCC1, we used RCC1 tagged with green fluorescent protein (RCC1-GFP). Binding of RCC1-GFP to sperm chromatin was detectable within 10 min after addition of the egg extract, but not the buffer alone (20). These data demonstrate that mobilization of RCC1 to chromatin occurs during stage I decondensation.

Decondensation may allow access to pre-existing RCC1-binding sites on DNA; alternatively, addition of egg lysate may create RCC1-binding sites by depositing H2A/H2B onto chromatin. To differentiate between these possibilities, we separated chromatin decondensation from H2A/H2B incorpora-

tion and observed RCC1-GFP binding (21). When treated with the buffer alone, sperm remained condensed (Fig. 3B). However, addition of nucleoplasmic core (NpIC) decondensed nuclei without promoting RCC1-GFP binding (Fig. 3, B and C). This evidence supports our conclusion that neither DNA nor endogenous H3/H4 are sufficient to dock RCC1 to chromatin (Fig. 3, B through D). When histones were added to condensed chromatin, a small increase of RCC1-GFP binding was observed. Fluorescence appeared in discrete foci along the chromatin periphery, suggesting that RCC1 could access only a fraction of the condensed chromatin. In contrast, treatment with NpIC plus histones produced a \sim 25-fold increase in RCC1-GFP binding. Purified H2A/H2B stimulated chromatin binding to a similar extent as the histone extract (14).

We next compared protein constituents of the chromatin under each experimental condition. By two-dimensional gel electrophoresis (17), the level of H2A/H2B deposition reflected the level of RCC1-GFP binding. In addition, binding of RCC1 occurred during the same time frame as H2A/H2B incorporation. Together, these data suggest that the interaction between RCC1 and chromatin requires the integration of histones H2A/H2B. This observation, together with both the binding exhibited by RCC1 for H2A/H2B in vitro and the stimulation of RCC1

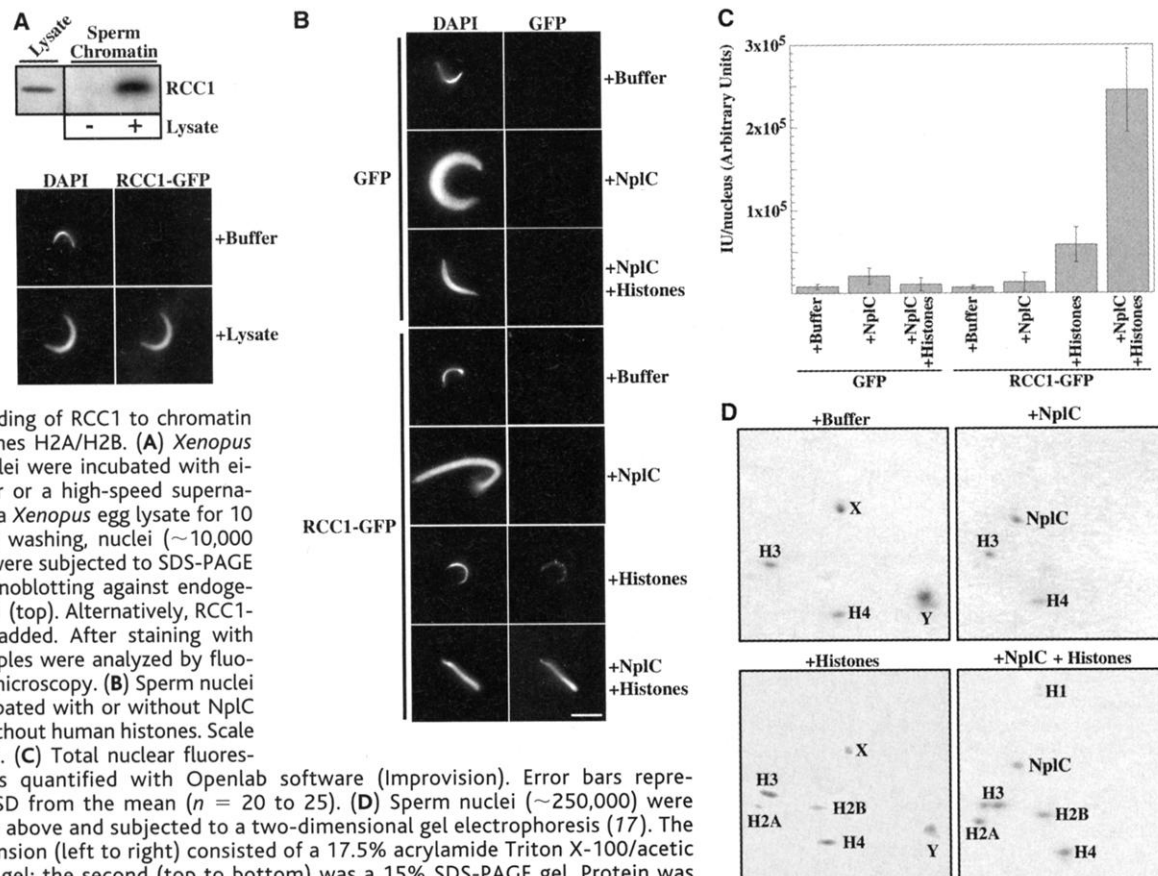


Fig. 3. Binding of RCC1 to chromatin uses histones H2A/H2B. (A) *Xenopus* sperm nuclei were incubated with either buffer or a high-speed supernatant from a *Xenopus* egg lysate for 10 min. After washing, nuclei (\sim 10,000 per lane) were subjected to SDS-PAGE and immunoblotting against endogenous RCC1 (top). Alternatively, RCC1-GFP was added. After staining with DAPI, samples were analyzed by fluorescence microscopy. (B) Sperm nuclei were incubated with or without NpIC with or without human histones. Scale bar, 5 μ m. (C) Total nuclear fluorescence was quantified with Openlab software (Improvision). Error bars represent \pm 1 SD from the mean ($n = 20$ to 25). (D) Sperm nuclei (\sim 250,000) were treated as above and subjected to a two-dimensional gel electrophoresis (17). The first dimension (left to right) consisted of a 17.5% acrylamide Triton X-100/acetic acid/urea gel; the second (top to bottom) was a 15% SDS-PAGE gel. Protein was stained with Coomassie.

Protective Role of ATP-Sensitive Potassium Channels in Hypoxia-Induced Generalized Seizure

Katsuya Yamada,^{1*} Juan Juan Ji,^{1*} Hongjie Yuan,¹ Takashi Miki,⁴ Shinichi Sato,¹ Naoki Horimoto,¹ Tetsuo Shimizu,² Susumu Seino,⁴ Nobuya Inagaki^{1,3†}

Adenosine triphosphate (ATP)-sensitive potassium (K_{ATP}) channels are activated by various metabolic stresses, including hypoxia. The substantia nigra pars reticulata (SNr), the area with the highest expression of K_{ATP} channels in the brain, plays a pivotal role in the control of seizures. Mutant mice lacking the Kir6.2 subunit of K_{ATP} channels [knockout (KO) mice] were susceptible to generalized seizures after brief hypoxia. In normal mice, SNr neuron activity was inactivated during hypoxia by the opening of the postsynaptic K_{ATP} channels, whereas in KO mice, the activity of these neurons was enhanced. K_{ATP} channels exert a depressant effect on SNr neuronal activity during hypoxia and may be involved in the nigral protection mechanism against generalized seizures.

K_{ATP} channels (1) couple the intracellular metabolic state to electrical activity at the plasma membrane (2). We have previously reported the molecular structure of K_{ATP} channels (3, 4) comprising the inwardly rectifying K^+ channel Kir6.2 and a sulfonylurea receptor with high affinity (SUR1 in pancreatic β cells) or low affinity (SUR2A in the heart) for sulfonylureas. High-affinity binding of [³H]glibenclamide in the brain is strongest in the SNr, suggesting high expression of the β cell type K_{ATP} channel in this nucleus (5, 6). Because the SNr acts as a central gating system in the propagation of seizure (7–9) and generalized seizures can be evoked by metabolic stresses such as hypoxia and hypoglycemia (10), these K_{ATP} channels could well be involved in the development of seizure during ATP-depleted conditions.

Kir6.2 KO mice (11) were used to evaluate this possibility. Daily behavior and basal physiological values of KO mice were not significantly different from those of wild-type mice (12, 13). However, responses to brief (150 s) hypoxia caused by oxygen deprivation ($n = 19$, $5.4 \pm 0.2\%$ O_2) differed in KO and wild-type mice (14). The wild-type mice (10/10) all remained sedated during the challenge and revived normally. In contrast, the KO mice all responded with a myoclonic

jerk (latency = 8.9 ± 1.1 s, $n = 9$) followed by severe tonic-chronic convulsion and death (survival time = 21.8 ± 5.2 s, $n = 9$) (Table 1). Under more severe hypoxic conditions ($n = 6$, $4.3 \pm 0.2\%$ O_2 , $P < 0.0001$ compared with $5.4 \pm 0.2\%$ O_2), four of the six wild-type mice exhibited a generalized convulsion (latency = 25.8 ± 2.7 s) (15). Electroencephalogram (EEG) and electromyogram (EMG) (14) revealed a sequence of seizure patterns in conscious KO mice ($n = 5$) challenged with $5.4 \pm 0.1\%$ O_2 (Fig. 1A). First, very low-voltage EEG for about 3 s indicated loss of consciousness. Then fast waves after an abrupt, sharp deflection lasted for several seconds in the EMG traces, corresponding to the tonic convulsion and myoclonus, after which bilateral, high-voltage sharp wave bursts were observed in the EEG traces. In wild-type mice under the same conditions, a medium- to low-voltage EEG predominated during the hypoxic period (Fig. 1B). This suggests that K_{ATP} channels participate in determining the seizure threshold during hypoxia. It is unlikely that the seizures observed in KO mice were produced by rapid cardiac arrest, because heartbeats continued after the seizure (16).

To investigate the role of SNr neuron activity, we recorded single unit activities from the SNr in acute slice preparations (17). In control, the firing rate of SNr neurons was not significantly different in wild-type and KO mice [25.2 ± 1.8 Hz ($n = 60$) and 22.6 ± 2.1 Hz ($n = 47$) for wild-type and KO mice, respectively]. However, in brief hypoxia (90 s) (18), wild-type neurons showed a marked decrease in firing rate to about one-third that before hypoxia (from 28.4 ± 2.0 Hz to 10.2 ± 3.2 Hz, $n = 9$, $P = 0.0003$; Fig. 2, A

by nucleosomes, strongly suggests that RCC1 binds H2A/H2B on chromatin, possibly at surfaces exposed on the faces of each nucleosome.

References and Notes

- M. Hetzer, D. Bilbao-Cortes, T. C. Walther, O. J. Gruss, I. W. Mattaj, *Mol. Cell* **5**, 1013 (2000).
- C. Zhang, P. R. Clarke, *Science* **288**, 1429 (2000).
- M. Dasso, *Cell* **104**, 321 (2001).
- D. Görlich, U. Kutay, *Annu. Rev. Cell Dev. Biol.* **15**, 607 (1999).
- H. Seino, N. Hisamoto, S. Uzawa, T. Sekiguchi, T. Nishimoto, *J. Cell Sci.* **102**, 393 (1992).
- C. A. Mizzen, J. E. Brownell, R. G. Cook, C. D. Allis, *Methods Enzymol.* **304**, 675 (1999).
- Recombinant proteins were prepared as described (22). Equal amounts of each GST-fusion protein were bound to glutathione-Sepharose (Pharmacia) then blocked in 5% bovine serum albumin/phosphate-buffered saline (w/v). Assays were carried out (in 20 mM 3-[N-morpholino]propanesulfonate, pH 7.1, 100 mM potassium acetate, 5 mM magnesium acetate, 1 mM dithiothreitol, and 0.05% Tween-20 (v/v)) for 60 min at 4°C with intact nucleosomes (6), trypsinized nucleosomes (23), purified chicken histones, or isolated H2A or H2B (Roche) (all 1 μ M or the indicated concentration). Where indicated, Ran, Ran(T24N), or Ran(Q69L) were added (10 μ M). Free histones were isolated on SP-Sephadex beads (Pharmacia). After washing both sets of beads, the proteins were eluted, subjected to SDS-polyacrylamide gel electrophoresis (SDS-PAGE), and stained with Coomassie.
- P. Cheung, C. D. Allis, P. Sassone-Corsi, *Cell* **103**, 263 (2000).
- M. E. Nemergut, I. G. Macara, unpublished data.
- V. Karantzis, E. Freire, E. N. Moudrianakis, *Biochemistry* **35**, 2037 (1996).
- F. R. Bischoff, C. Klebe, J. Kretschmer, A. Wittinghofer, H. Ponstingl, *Proc. Natl. Acad. Sci. U.S.A.* **91**, 2587 (1994).
- C. Klebe, F. R. Bischoff, H. Ponstingl, A. Wittinghofer, *Biochemistry* **34**, 639 (1995).
- S. A. Richards, K. M. Lounsbury, I. G. Macara, *J. Biol. Chem.* **270**, 14405 (1995).
- Supplementary material is available on Science Online at www.sciencemag.org/cgi/content/full/292/5521/1540/DC1.
- A. W. Murray, *Methods Cell Biol.* **36**, 581 (1991).
- A. Philpott, G. H. Leno, R. A. Laskey, *Cell* **65**, 569 (1991).
- A. Philpott, G. H. Leno, *Cell* **69**, 759 (1992).
- M. Dasso, H. Nishitani, S. Kornbluth, T. Nishimoto, J. W. Newport, *Mol. Cell Biol.* **12**, 3337 (1992).
- G. H. Leno, *Methods Cell Biol.* **53**, 497 (1998).
- Xenopus* sperm nuclei (10^5 /ml) were incubated in a high-speed supernatant from a *Xenopus* egg lysate or in sperm buffer [20 mM Hepes (pH 7.7), 100 mM KCl, and 1 mM MgCl₂] for 10 min (15). After washing, chromatin-bound proteins were eluted, subjected to SDS-PAGE, and immunoblotted with anti-*Xenopus*-RCC1 serum. Alternatively, RCC1-GFP (500 nM) was added to the above reactions. Samples were treated with formaldehyde and 4',6'-diamidino-2-phenylindole (DAPI) and analyzed immediately by fluorescence microscopy.
- Xenopus* sperm nuclei (10^5 /ml) were incubated in sperm buffer with or without NpIC (1 mg/ml) for 10 min at 25°C. The indicated GFP fusion protein (500 nM) was added with or without human histones (1 mg/ml) for 10 min at 25°C. Samples were fixed, stained, and analyzed (20). Where indicated, the GFP-fusion proteins were omitted and the nuclei were subjected to a two-dimensional gel analysis (17).
- M. E. Nemergut, I. G. Macara, *J. Cell Biol.* **149**, 835 (2000).
- A. E. de la Barre et al., *EMBO J.* **19**, 379 (2000).
- C. Klebe, H. Prinz, A. Wittinghofer, R. S. Goody, *Biochemistry* **34**, 12543 (1995).
- We thank M. Dasso for providing the anti-*Xenopus*-RCC1 serum, D. Görlich for the NpIC and BIB expression vectors, and T. Nishimoto for the RCC1 cDNA. Supported by grant GM-50526 from NIH, Department of Health and Human Services.

¹Department of Physiology and ²Department of Psychiatry, Akita University School of Medicine, and ³CREST of Japan Science and Technology Cooperation (JST), 1-1-1, Hondo, Akita 010-8543, Japan. ⁴Department of Cellular and Molecular Medicine, Graduate School of Medicine, Chiba University, 1-8-1 Inohana Chuo-Ku, Chiba 260-8670, Japan.

*These authors contributed equally to this work.

†To whom correspondence should be addressed: E-mail: inagaki@med.akita-u.ac.jp

21 February 2001; accepted 10 April 2001